

## Fabrication and Characterization of Superconducting Nano Layer by Pulsed Laser Deposition

Badr Y.A.<sup>a</sup>, M. I. Youssif<sup>fb,\*</sup>, Tharwat El-Sherbini<sup>c</sup>, and D. Hassan<sup>a</sup>

<sup>(a)</sup> Department of Laser Interaction with Matter, NILES, Cairo University, Giza, Egypt

<sup>(b)</sup> Physics Department, Faculty of Science, Damietta University, New Damietta 34517, Egypt

<sup>(c)</sup> Physics Department, Faculty of Science, Cairo University, Giza, Egypt

\*[youssifm@yahoo.com](mailto:youssifm@yahoo.com)

**Abstract:** Pulsed laser deposition (PLD) technique based on femtosecond (*f.s.*) provide with 2 amplifiers was used to fabricate nano layer of YBCO thin superconducting films on a quartz substrate. A femtosecond laser contains to Ti: sapphire crystal is pumped by 2<sup>nd</sup> harmonic of Nd:YLF laser at 523 nm. The femtosecond laser was focused on a rotating target and was made incident on the target surface at an angle of 45°. The substrate temperature was kept at 400°C and the films were deposited in vacuum and in the presence of pure oxygen at a pressure ( $P_{O_2}$ ) of  $5.5 \times 10^{-5}$  Torr using turbo molecular pump. In the present study, we have varied the distance from the target to the substrate ( $d_{T-S}$ ) in order to improve the film quality. As a result, we have achieved both of high quality films and the uniformity in deposition rate under the optimized condition of  $d_{T-S} = 70$  mm. Nano-layer of superconducting films are identified as  $Y_2Ba_5Cu_7O_x$  and  $Y_2Ba_4Cu_8O_{20-x}$ , respectively, as revealed by XRD and EDX measurements. Thickness of the films was measured by Fizeau interference (*FI*) technique at reflection and found to be ~150 nm with a deposition time of 10 min. Atomic force microscope scans, recorded in a tapping mode, of  $Y_2Ba_4Cu_8O_{20-x}$  thin film surface shows that the film start to have some atomic arrangements after laser ablation treatment with grain size of 100-300 nm. Resistivity measurements for the target superconductor  $Y_1Ba_2Cu_3O_{6.96}$  revealed a transition temperature  $T_c^{onset} = 90$  K with a transition width  $\Delta T_c = 2.0$  K and the zero resistance is achieved at  $T_c(0) = 88$  K. The Raman spectra of YBCO indicate that the five z-polarized Raman phonons exist. The electrical and structural studies of the polycrystalline and PLD-YBCO nano-superconducting layer films were determined in details by employing structural x-ray diffraction (XRD), scanning electron microscope (SEM), energy-dispersive X-ray spectroscopy (EDX), atomic-force microscope (AFM), as well as the electrical resistance R(T) measurements. Additionally, Raman spectroscopy was used to obtain more information about texture, in particular oxygen content, the detection of foreign phases, and orientation of YBCO superconducting material. Finally, we have investigated the fluorescence of the films using an ultraviolet light source. By using PLD technique, we can fabricate films of nano superconducting layers with the same chemical structure as the target material. This information would be useful particularly in the fabrication of high  $T_c$ -device.

[Badr Y. A., M. I. Youssif, Tharwat El-Sherbini, and D. Hassan. **Fabrication and Characterization of Superconducting Nano Layer by Pulsed Laser Deposition.** *Life Sci J* 2016;13(5):8-20. ISSN: 1097-8135 (Print) / ISSN: 2372-613X (Online). <http://www.lifesciencesite.com>. 2. doi:[10.7537/marslsj13051602](https://doi.org/10.7537/marslsj13051602).

**Index Terms:** Pulsed laser deposition; Superconducting Nano-layer films; YBCO; SEM; AFM; Raman spectroscopy, Fluorescence

### 1. Introduction

High-Tc superconducting (HTSC) thin films  $Y_1Ba_2Cu_3O_{7-\delta}$  (YBCO or Y123) on low dielectric loss substrates are suitable candidates for applications as passive microwave devices in the future communication systems. There is a huge number of activities to develop microwave devices using HTSC thin films, because in this field real market applications of HTSC subsystems seem to be possible in the nearest future. For satellite communication systems [1-3], devices like microwave strip line filters require HTSC thin films on both sides of large-area crystal wafers.

In thin film growth technology, various techniques, namely chemical and physical methods, have been developed for the deposition of thin film superconductors. The chemical method is composed of metal organic chemical vapour deposition (MOCVD)

[4, 5], metal organic deposition (MOD) - solution methods [6, 7] and liquid phase epitaxy (LPE) [8, 9]. The physical method consists of the magnetron sputtering, pulsed laser deposition (PLD) and the co-evaporation method. Several groups[10] have successfully deposited superconductive  $Y_1Ba_2Cu_3O_{7-x}$  coatings by MOCVD on different substrate materials with high critical current densities in applied magnetic fields [11-13]. However, the rougher film surface and larger surface resistance are the disadvantages of this method. Preparation of some oxide films as e.g. strontium titanium STO [14], barium zirconate which can act as buffer layers, and of Y123 films have been reported by using MOD-solution methods [15-17]. The advantages of this method over other deposition techniques are rapid deposition rates and the simplicity with which films of uniform and controlled

composition can be prepared. Although the MOD solution methods greatly reduce the production cost they rarely obtain high  $J_c$  over  $1 \text{ MA/cm}^2$  (77 K, 0 T). The LPE method has the advantage in the ability to fabricate a thick superconducting layer of YBCO and other rare earth cuprate (ReBCO) [18-20]. Nevertheless, still some disadvantages include poor surface finish; poor large area uniformity and difficulty in varying stoichiometry have been reported [21]. The magnetron sputtering method has been widely used for  $\text{MgB}_2$  [22] and YBCO [23] thin films depositions because of their high deposition rates and relatively low temperature process conditions. Anyway, the critical current densities  $J_c$  of YBCO films grown by sputtering are still lower than films prepared by pulsed laser deposition (PLD). However, it still remains a major challenge for most thin film groups to optimize the deposition method to produce high quality films.

Pulsed laser deposition (PLD) is a thin film deposition (specifically a physical vapor deposition, PVD) technique where a high power pulsed laser beam is focused inside a vacuum chamber to strike a target of the material that is to be deposited. This material is vaporized from the target (in a plasma plume) which deposits it as a thin film on a substrate (such as sapphire, quartz, silicon wafer facing the target). This process can occur in vacuum or in the presence of a background gas, such as oxygen which is commonly used when depositing oxides to fully oxygenate the deposited films. PLD is becoming one of the most important techniques to engineer thin film growth in research laboratories, because it has significant advantages over most other deposition processes, including the capability for stoichiometric transfer of material from target to substrate, low contamination level, high deposition rate and non-equilibrium processing conditions. PLD is considered the most convenient and efficient technique for the synthesis of high quality films of HTSC thin films. Furthermore, the method is relatively easily, fast and the capital cost involved is low, as well. Recently, the PLD technique has been applied successfully to deposit thin films of  $\text{Y}_1\text{Ba}_2\text{Cu}_3\text{O}_{7-x}$  [24-27],  $\text{Yb}_1\text{Ba}_2\text{Cu}_3\text{O}_7$  [28],  $\text{Ho}_1\text{Ba}_2\text{Cu}_3\text{O}_{7-x}$  [26],  $\text{Gd}_1\text{Ba}_2\text{Cu}_3\text{O}_{7-x}$  [29] and  $\text{La}_{1.85}\text{Sr}_{0.15}\text{CuO}_{4-x}$  [30] of the high- $T_c$  oxide superconductors. The 1:2:3 stoichiometry of the target material (usually a bulk superconducting pellet) can be reproduced relatively easily in the films, to within about 10%. However, at low laser energy densities, deficiencies of yttrium have been reported [31, 32].

In high- $T_c$  cuprate superconductors, the structural differences, the number of  $\text{CuO}_2$  planes and CuO chains lead to various physical properties and critical temperatures  $T_c$ . YBCO-family compounds like Y123 has two  $\text{CuO}_2$  planes and one CuO chain, exhibiting a  $T_c$  in the 92-94 K range; whereas, Y124 compounds

have one  $\text{CuO}_2$  plane and one double CuO chain, featuring a  $T_c \approx 80 \text{ K}$  [33]. Recently, Y358 (a new member of the YBCO family) has been found to have five  $\text{CuO}_2$  planes and three CuO chains with  $T_c \geq 100 \text{ K}$  [34]. The improvement in  $T_c$  has been attributed to the lower number of holes in the CuO chains of Y358 and Y247 relative to Y123 and Y124 superconductors [35]. In the  $\text{La}_2\text{CuO}_4$  compound there is one  $\text{CuO}_2$  plane, but the Y123 structure has two  $\text{CuO}_2$  planes and one chain. It has been found that by limited increase in the number of the  $\text{CuO}_2$  planes in all high- $T_c$  cuprate superconductors to three, the superconducting transition temperature increases [36].

In the present work, we describe the fabrication of superconducting nano-layer films of YBCO on a quartz substrate by using the pulsed laser deposition (PLD) method based on femtosecond (*f.s.*) in vacuum and in the presence of oxygen atmosphere at a given pressure, to fully oxygenate the films, at a low deposition temperature of  $400 \text{ }^\circ\text{C}$ . All samples were characterized in detail by employing structural XRD, SEM, EDX and AFM as well as the electrical (R-T) measurements. Furthermore, Raman spectroscopy and fluorescence were investigated. The experiment and the results will be detailed below.

## 2. Experimental Techniques

Superconductor pellet of  $\text{Y}_1\text{Ba}_2\text{Cu}_3\text{O}_{7-\delta}$  bulk sample was prepared by a conventional solid state reaction method [37]. Briefly, the ingredients of  $\text{Y}_2\text{O}_3$ ,  $\text{BaCO}_3$  and  $\text{CuO}$  of 99.99% purity were thoroughly mixed in required proportions and calcined at  $910^\circ\text{C}$  in air for a period of 24 h. This exercise was repeated three times with intermediate grinding at each stage. The resulting powders were ground, mixed, palletized and annealed in flowing oxygen at a  $960^\circ\text{C}$  for a period of 24 h and then furnace cooled to room temperature with an intervening annealing for 24 h at  $600 \text{ }^\circ\text{C}$ . The second pellet was annealed at  $460 \pm 5^\circ\text{C}$  in flowing argon for 20 h and then quenched to room temperature in order to reduce the oxygen content. The oxygen content ( $\delta$ ) of the prepared samples was found to be 6.964 and 6.78, respectively, as determined by the iodometric titration method [38, 39]. This pellets were used as a targets for the deposition of superconducting nano-layer films.

A good foundation for versatile PLD system is comprised of laser source (to ablate material from the face of a superconducting pellet onto a nearby substrate), deposition chamber, target manipulation, substrate and/or heater, and vacuum system. Figure 1 shows a schematic diagram of the experimental setup. PLD techniques based on femtosecond (*f.s.*) provide with 2 amplifiers (800 nm, 40 *f.s.* pulses duration, 1000 Hz repetition rates, 0.3–0.75 mJ) was used to deposit YBCO superconducting nano-layer films on a quartz

substrates (10×10×1mm). The Quartz substrates have the advantages of modest dielectric constant and good thermal expansion as well. A femtosecond laser (Egyptian National Research Center) contains Ti:sapphire crystal is pumped by 2<sup>nd</sup> harmonic of Nd:YLF laser at 523 nm. The obtained beam is mode locked to give pulse 40f.s.at a central wave length 800 nm with a pulse frequency of 1KHZ. Then two optical amplifiers had been used. This system is composed of pulse stretcher, regenerative amplifier. The femtosecond laser was focused on rotating target. The target was mounted in a deposition chamber of cylindrical shape (Johnsen-ultravaci NC) which could be evacuated to a base pressure of 1×10<sup>-6</sup> Torr. The chamber has typically a large number of ports (8 ports), for pumping system, gas inlets, pressure monitoring, etc. Femtosecond laser was used for ablation and it was made incident on the target surface at an angle of 45°. Target of disk-shaped (typically 10×1.5 mm) was mounted on a stainless-steel holder to keep the ablation target fixed in the vertical orientation during the deposition process. The laser beam scanned over the surface of the flat target to provide uniform erosion, this has the advantages of moving the plume relative to the substrate. The target was slowly rotated (about the vertical axis) relative to the incoming laser beam (10 rpm) during deposition to reduce target texture resulting from repeated ablation at the same site. Alternately the target assembly can house an (x-y) translation stage as well. A stepper motor was used so that the target stepped in both the X and Y-direction while the laser interaction spot is held stationary and so the target surface area can be used more effectively for a longer duration without groove formation.

The depositions of YBCO films have been occurred in vacuum and in the presence of oxygen atmosphere at a pressure of 5.5×10<sup>-5</sup> Torr, to fully oxygenate the films, using turbo molecular pump. In this study, we have varied the distance from the target to the substrate ( $d_{T-S}$ ) in order to improve the film quality. The substrate was mounted in front of the target at a distance of 20 mm, 40 mm and 70 mm. The substrate temperature was typically maintained at 400°C by using halogen lamp to allow surface mobility of the deposited species while limiting oxygen out-diffusion. The quoted temperature was measured by placing the thermocouple on the substrate surface itself. The estimated inaccuracy of the temperature measurement reported here is about ± 20°C. This low temperature is compatible with semiconductor device processing technology and also reduces film contamination due to substrate diffusion.

In the present work, Thin Film Thickness is measured by Fizeau Interferometer ( $F_I$ ) technique at reflection. This technique provides a field of sharp dark lines with bright background, Figure 2. When thin film

sheet is inserted between Fizeau plates, one can notice a shift in the dark lines ( $\Delta h$ ). This shift gives a good measurement of the film thickness. The film thickness ( $t$ ) can be calculated from the fringe patterns shown in Fig. 2 by using the following equation [40]:

$$t = \left(\frac{\lambda}{2}\right) \left(\frac{\Delta h}{h}\right) \quad (1)$$

where  $\lambda$  is the wavelength of the used light and  $h$  is the fringe spacing. The film thickness was found to be ~150 nm with a deposition time of 10min. The phase purity of the deposited films were characterized by X-ray powder diffraction (Bruker D8 Advance) in the angle range  $2\theta = 5 - 90^\circ$  at room temperature using Cu  $K_\alpha$  radiation and graphite monochromator ( $\lambda=1.5411$  nm) powered at 40 KV and 40 mA. The scanning speed was 10°/min and the scanning angular range was between 100 and 500. The electrical resistivity of the samples is obtained by using the standard four-probe technique in closed cycle refrigerator [Cryo-compressor Model 531-120-IBARA working with helium] within the range of (15– 300 K). Digital nano voltmeter (Model 182-KEITHLEY) was used to measure the voltage drop across the sample. A programmable current source (Model 224-KEITHLEY) with current range from 1 mA to 100 mA and temperature controller (Lakeshore Model321) supplied with silicon diode thermocouple and heating element with accuracy of ± 0.1° are used during these measurements. Temperatures were measured with a calibrated Pt resistance thermometer and the contacts were made with the help of conducting silver paint. The microstructure and surface morphology studies of the PLD-YBCO superconducting nano-layer films were determined in details by employing scanning electron microscope (SEM) micrographs and energy-dispersive X-ray (EDX) analysis as well as atomic-force microscope (AFM). The SEM model Philips XL-30SFEG equipped with EDX unit (Material Geological Research Center, Egypt), accelerating voltage 30 KV, magnification up to 400,000x, and resolution for W (3.5 nm) have been used for this investigation. All samples were coated with carbon. In addition, AFM (CP-II Veeco, USA) was used to investigate the morphology of the deposited films. Finally, Raman spectroscopy was used in an effort to obtain information about the vibrational structure of atoms in YBCO superconductors.

### 3. Results and Discussion

#### 3.1. Characterization of the bulk YBCO superconducting target

X-ray diffraction analysis using Cu $K_\alpha$  radiation, at room temperature, was carried out to identify the

crystal structure of the prepared target. Figure 3 shows the XRD spectrum of the superconducting  $Y_1Ba_2Cu_3O_{6.78}$  bulk sample in the angle range  $2\theta = 5-90^\circ$ . It is clear that  $Y_1Ba_2Cu_3O_{6.78}$  has an orthorhombic structure as being evident from the crystallographic splitting of (013), (103)/ (110), and (020), (006), and (116)/ (123), (213). In addition to the difference in peak heights around  $32.58^\circ$  is clearly seen. In the orthorhombic phase the intensity of (013) peak is less than (103)/ (110) peak [41]. The peaks of (001) reflections shown in X-ray figure indicates that the target is c-axis oriented. The oxygen stoichiometry of the target is determined by iodometric titration method.

Figure 4 shows the results of resistivity measurements on orthorhombic superconducting  $Y_1Ba_2Cu_3O_{6.964}$  compound from room temperature down to 15K. This figure shows that the orthorhombic phase is metallic with small resistivity which decreases linearly with decreasing temperatures. It shows deviation from linearity beginning around 100K. In going to the superconducting state, a sharp drop in resistivity occurs at a transition temperature  $T_c^{onset} = 90$  K with a transition width  $\Delta T_c = 2.0$  K. The zero resistance is achieved at  $T_c(0) = 88$  K in agreement with the published results [42]. For the elemental microanalysis, Energy-dispersive X-ray spectroscopy (EDX) was used to identify the chemical contents of the prepared superconducting target. EDX spectrum represented in Figure 5 shows only O, Cu and Y peaks caused by X-rays given off as electrons return to the K electron shell and one peak resulting from the L shell of Ba. No undesired phases were detected confirming that the target structure is an orthorhombic single phase.

Most HTSC are Centro symmetric crystals. Their elementary excitations (phonons) are either odd or even. Raman spectroscopy involving two photons (each of them odd) only couples to even excitations. IR spectroscopy involves only one photon and couples therefore only odd excitations exist. Almost all aspects of high- $T_c$  superconductivity have been addressed by Raman scattering because of its experimental versatility and the coupling of the elementary excitations to electron-hole pairs. In this work, Raman spectroscopy was used to obtain more information about texture, in particular oxygen content and the detection of foreign phases in YBCO superconducting sample [3]. This information would be useful particularly in the fabrication of high  $T_c$ -device. Figure 6 represents Raman spectra of  $Y_1Ba_2Cu_3O_{6.964}$  of the high- $T_c$  oxide superconductors. Referring to Figure 6, the appearance of peaks in the region marked by (1) at the frequency  $115\text{ cm}^{-1}$  indicates mainly the vibrations of the heaviest Barium atom (Ba), while the vibrations at  $150\text{ cm}^{-1}$  frequency (Peak marked by 2) involving those of the copper atoms Cu(2). The remaining three

modes marked by (3), (4) and (5) are dominated by vibrations of O(2) and O(3) oxygen atoms at  $340$  and  $440\text{ cm}^{-1}$  frequencies, respectively [43,44]. These frequencies have been found to be particularly sensitive to micro structural factors such as oxygen stoichiometry ( $7-\delta$ ) as well as the orientation of YBCO crystallites with respect to the polarizations of the incident and scattered laser beams [3,34]. Finally, the peak marked by (5) at the frequency  $500\text{ cm}^{-1}$  represents the vibration of the apical oxygen O(4) atoms toward the Cu(1) atom, parallel to the c-axis. The position of this peak has a linear variation with oxygen contents, and its position is often used to provide a measurement of ( $7-\delta$ ) [3, 33, 34]. This measurement is in good agreement with the results of oxygen stoichiometry determined by the iodometric titration method. Finally, the five z-polarized Raman phonons exist for the YBCO or thorbombic structure. Raman spectroscopy is a sensitive tool for detecting the composition, in particular oxygen content, the detection of foreign phases, and orientation of HTSC materials.

### 3.2. Characterization of the PLD-YBCO superconducting thin films

PLD techniques based on femtosecond (*f.s.*) provide with 2 amplifiers ( $800\text{ nm}$ ,  $40\text{ f.s.}$  pulses duration,  $1000\text{ Hz}$  repetition rates,  $0.3-0.75\text{ mJ}$ ) is used to deposit superconducting YBCO nano-layer thin films on a quartz substrates ( $10\times 10\times 1\text{ mm}$ ). The Quartz substrates have the advantages of modest dielectric constant and good thermal expansion as well. The substrate was mounted in front of the target at a distance of  $\sim 7\text{ cm}$  and it was heated up to a temperature of  $400^\circ\text{C}$  by using halogen lamp to allow surface mobility of the deposited species while limiting oxygen out-diffusion. The measured film thickness is  $\sim 150\text{ nm}$  as determined by *FI*-technique with a deposition time of  $10\text{ min}$ . After that, the nano-films were characterized in detail by employing structural XRD, SEM, EDX and AFM, as well as the electrical (R-T) measurements. X-ray diffraction analysis at room temperature using  $\text{CuK}\alpha$  radiation was carried out to identify the crystalline structure and orientation of the deposited films. Figure 7 shows the XRD patterns of the deposited YBCO films of thickness  $\sim 150\text{ nm}$  on a quartz substrates at  $400^\circ\text{C}$  without post-annealing (Figure 7a), and with an *ex-situ* annealing in a flow rate of a pure oxygen, for oxygenation, at  $950^\circ\text{C}$  for  $18\text{ h}$  (Figure 7b). The crystalline structure of the PLD nano films are identified as  $Y_2Ba_5Cu_7O_x$  and  $Y_2Ba_4Cu_8O_{20-x}$ , respectively. As can be seen, XRD indicates that the films are oriented mostly with the c-axis perpendicular to the substrate surface. The critical temperature was ranging from  $74$  to  $78\text{ K}$  and from  $81$  to  $83\text{ K}$ , respectively. A chemical microanalysis technique (EDX) was used to identify the chemical contents of the ablated PLD films. EDX spectrum

shown in Figure 8 confirmed the absence of impurity phases in the films. The analysis shows only O, Cu and Y peaks caused by X-rays given off as electrons return to the K electron shell and one peak resulting from the L shell of Ba. The PLD technique has the capability for texture transfer of material from target to substrate, low contamination level, high deposition rate and non-equilibrium processing conditions.

The proper target to substrate distance ( $d_{T,S}$ ) is very important for YBCO films grown by the PLD technique in order to improve the material yield. A scanning electron microscope (SEM) is a type of electron microscope that produces images of a sample by scanning it with a focused beam of electrons. The electrons interact with atoms in the sample, producing various signals that can be detected and that contain information about the sample's surface morphology and composition. Figure 9 shows SEM micrographs of  $Y_2Ba_4Cu_8O_{20-x}$  thin film surface, deposited at different target-substrate distance ( $d_{T,S}$ ) of 20 mm, 40 mm and 70 mm, respectively. The film was over coated with an ultrathin coating of gold to prevent surface charging. The white particles with a round shape in the photos (figure 9a and b) at  $d_{T,S} = 20$  mm are droplets which are typically observed in the film surfaces prepared by PLD technique [26, 45]. These droplets come from the drawback of PLD. During the ablation process of PLD, it is easy to eject micro-size particles from the target. If the target-substrate distance is not enough, those micro-size particles will deposit on the substrate and form those droplets as shown in the micrograph. The film deposited at  $d_{T,S} = 40$  mm contains a typical features for thick films as a flower-like shapes made of particulates rich in  $BaCuO_2$ , Ba and Cu-oxides [44]. In contrast, a dense smoother surface structure in a unique orientation was observed (Figure 9d) for the film deposited under the optimized condition of  $d_{T,S} = 70$  mm.

Atomic force microscopy (AFM) is a very high-resolution type of scanning (SPM), provides atomic or near-atomic-resolution surface morphology, which is ideal for determining angstrom-scale surface roughness on a sample. The surface imaging was investigated in a tapping mode, with  $512 \times 512$  data acquisitions at scan speed of 1.4 Hz at room temperature. Oxide-sharpened silicon nitride tips with integrated cantilevers with a nominal spring constant of 0.38 N/m were used. AFM images of  $Y_2Ba_4Cu_8O_{20-x}$  thin film growth on Quartz surface were investigated after treatment with laser ablation (Figure 10). The surface of the Quartz substrate with some aggregated features was found on the clean film which indicated that the surface was not well cleaned (Figure 10a). Higher resolution of this image is given in the inset with scan area of  $2 \times 2 \mu\text{m}$ . After laser ablation treatments, surface imaging of  $Y_2Ba_4Cu_8O_{20-x}$  film shows more irregularities with new protuberances which were not observed in the clean membrane surface. However, the film starts to have some atomic arrangements or assembly after laser ablation treatment as shown in the inset of figure 10b at a high resolution. The particles grain size is found to be 100-300 nm as estimated from AFM line profile.

Finally, the fluorescence of  $Y_2Ba_4Cu_8O_{20-x}$  thin film has been investigated by using an ultraviolet light source as shown in Figure 11. This figure shows the emission of a spectral line at a wavelength of  $\sim 830$  nm in the I.R region, due to the U.V irradiation of the surface of the superconductor thin film. Therefore, we can gather conclude that this emission line at a particular wavelength ( $\sim 830$  nm) is considered as an identification line for this type of HTSC thin films. Based on that fact, this property could be used as a finger print characterizing the deposited oxide thin superconducting films.

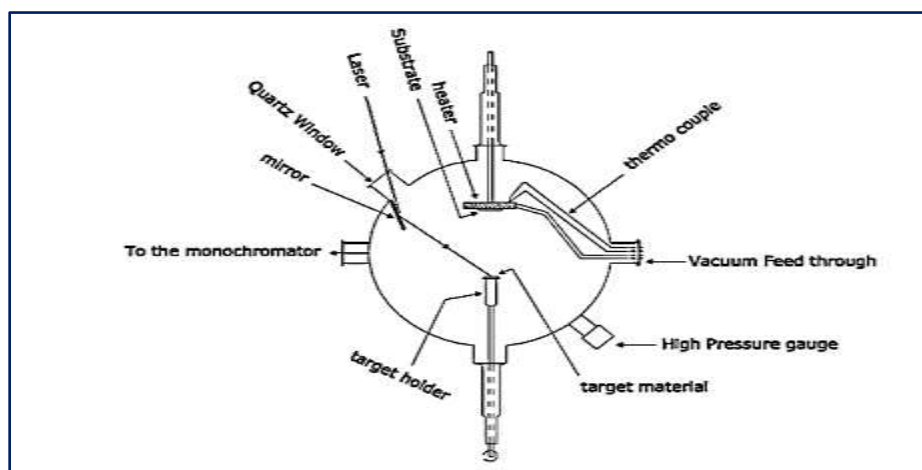


Figure 1. Schematic diagram of the PLD system.

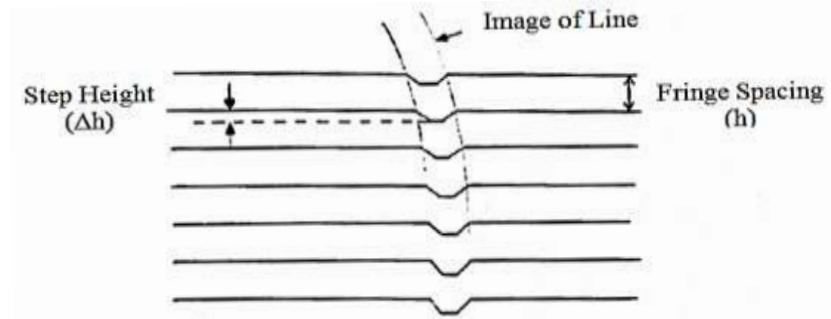


Figure 2. Fizeau fringe shifts at reflection for thin film thickness measurement.

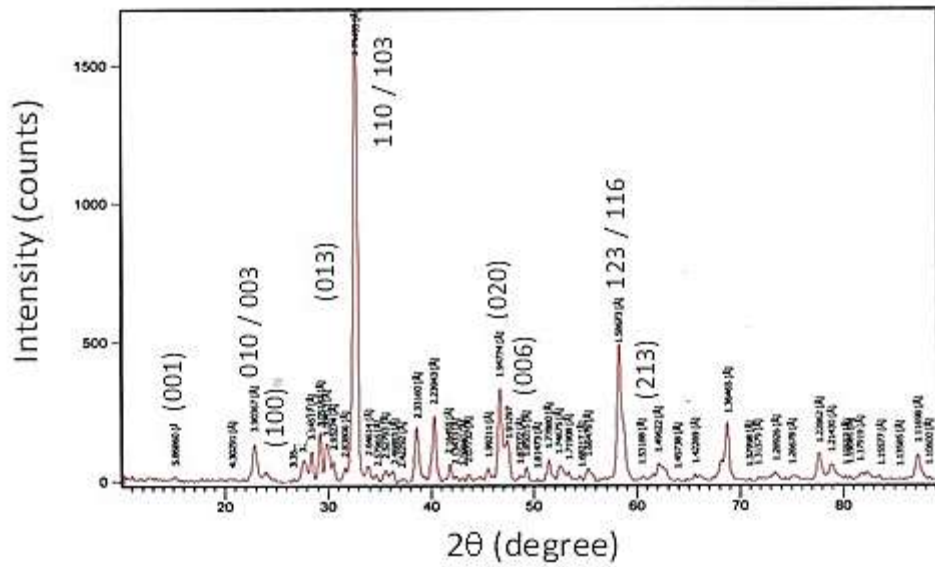


Figure 3. X-ray diffraction pattern of orthorhombic superconducting  $Y_1Ba_2Cu_3O_{6.78}$  sample. Intensity of (013) peak is less than (103)/ (110) peak.

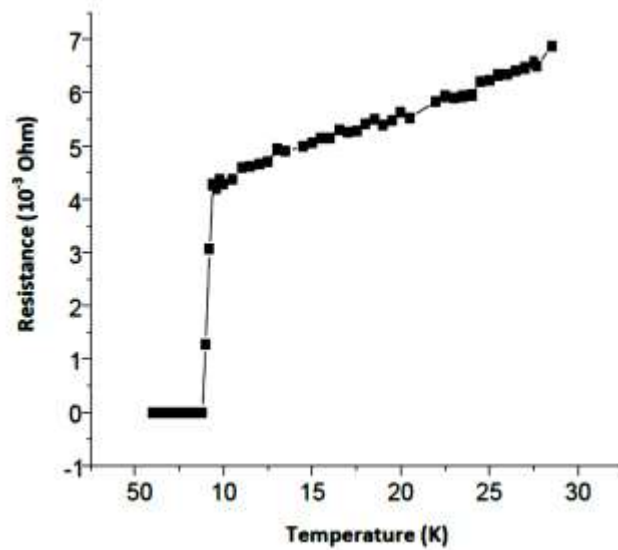


Figure 4. Plot of resistance versus temperature for orthorhombic superconducting  $Y_1Ba_2Cu_3O_{6.964}$  target.

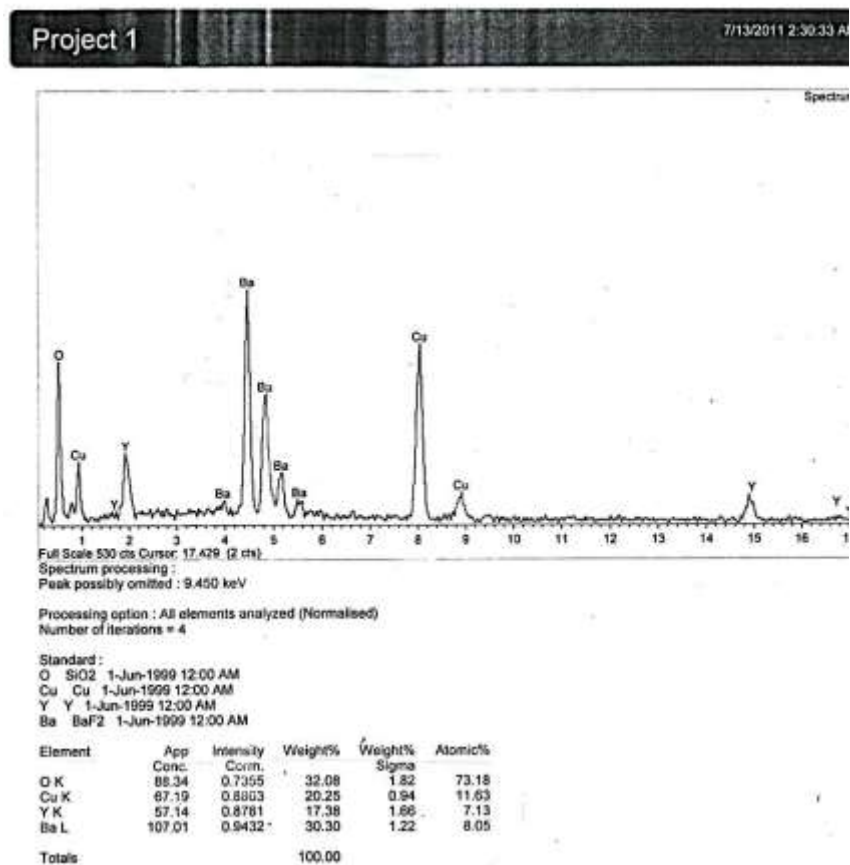


Figure 5. EDX spectrum of  $Y_1Ba_2Cu_3O_{6.964}$  superconductor target.

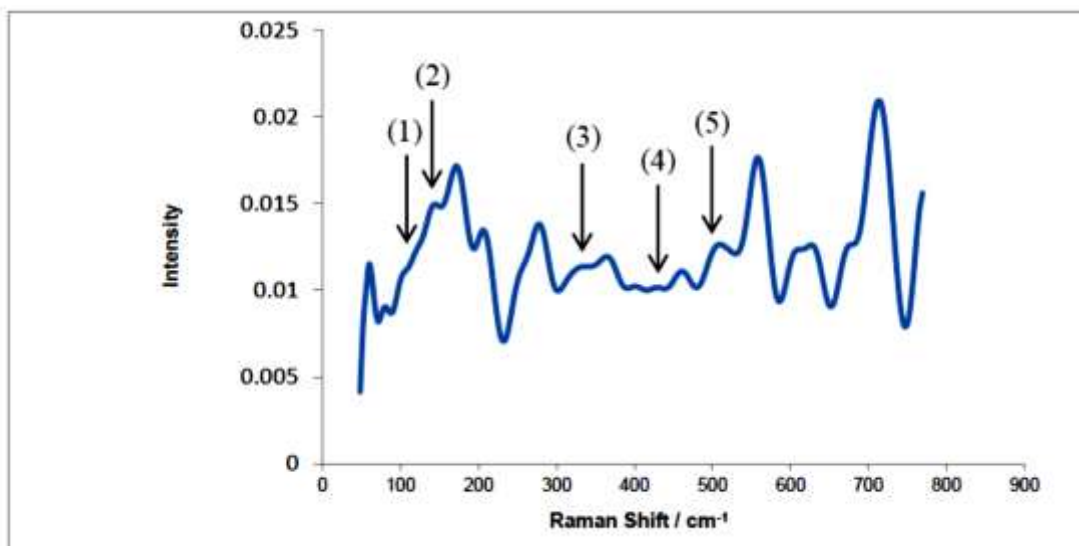


Figure 6. Raman microprobe spectra of  $Y_1Ba_2Cu_3O_{6.964}$  bulk superconductor.

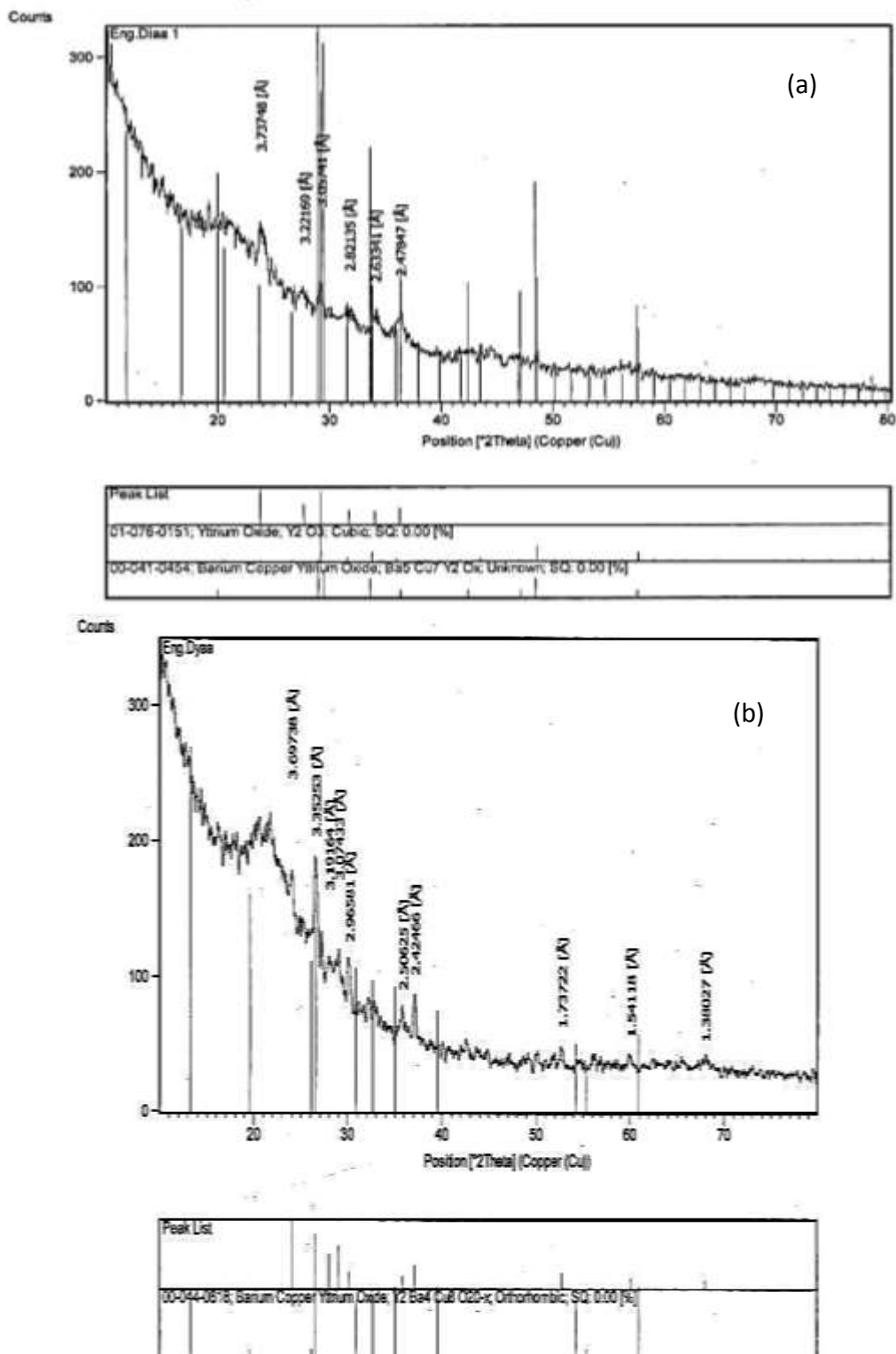


Figure 7. X-ray diffraction patterns for the PLD nano-films of:(a)  $Y_2Ba_5Cu_7O_x$  thin film deposited at  $400^\circ C$  without post-annealing, and (b)  $Y_2Ba_4Cu_8O_{20-x}$  thin film deposited at  $400^\circ C$  followed by an *ex-situ* annealing in a flow rate of pure oxygen, as described in the text.

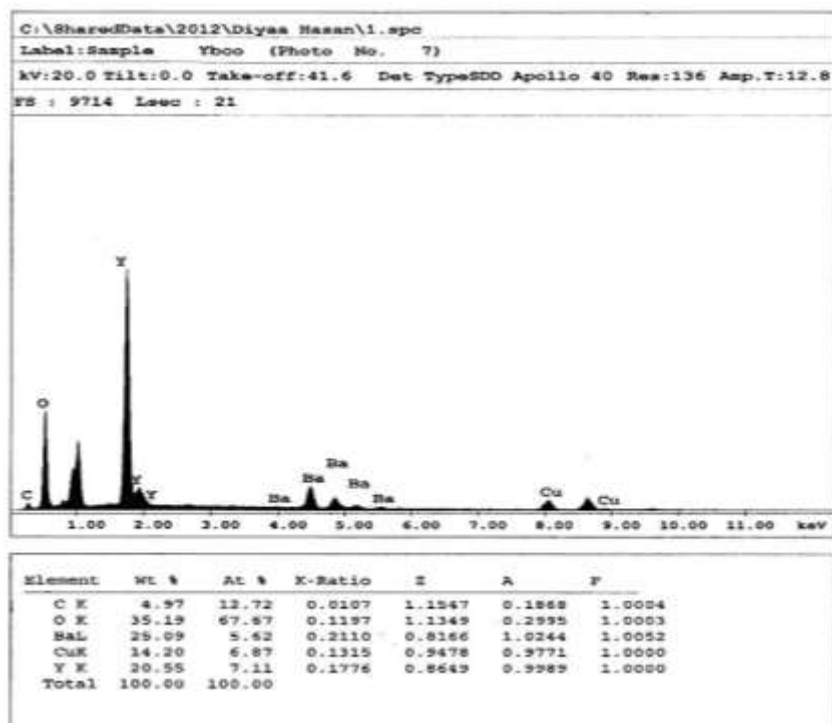


Figure 8. EDX analysis of the deposited  $Y_2Ba_4Cu_8O_{20-x}$  thin film.

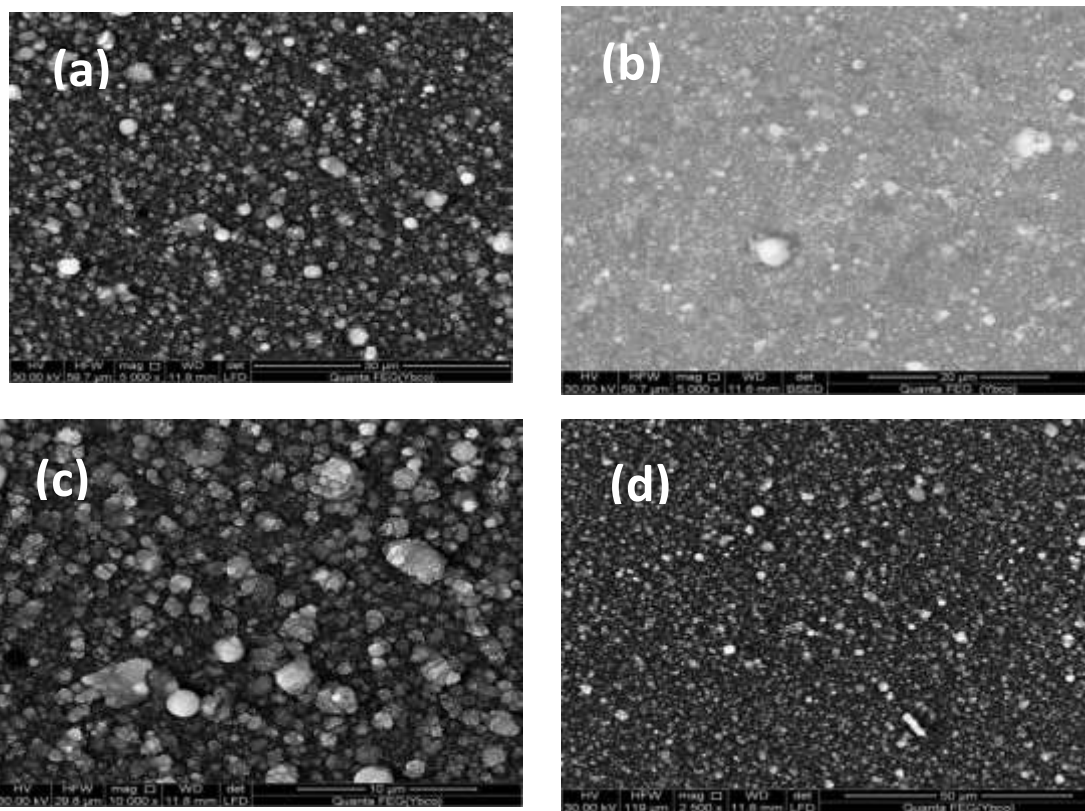


Figure 9. SEM micrographs of the surface of  $Y_2Ba_4Cu_8O_{20-x}$  thin film deposited by PLD technique at different target-substrate distance ( $d_{T-S}$ ) of: (a, b)  $d_{T-S} = 20$  mm, (c)  $d_{T-S} = 40$  mm, and (d)  $d_{T-S} = 70$  mm. The film was over coated with an ultrathin coating of gold to prevent surface charging.

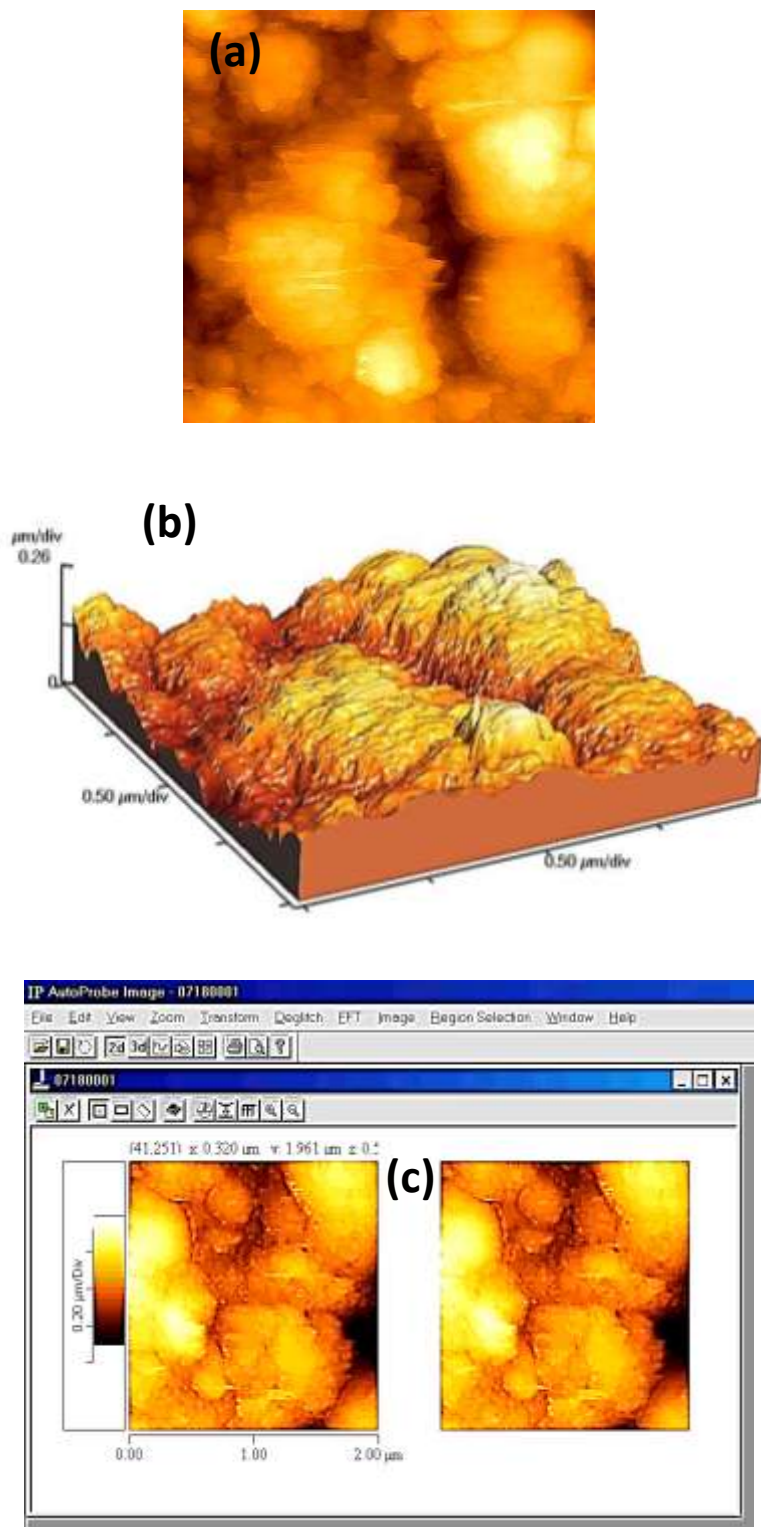


Figure 10. Atomic force microscope scans of  $\text{Y}_2\text{Ba}_4\text{Cu}_8\text{O}_{20-x}$  thin film surface. The micro and nano-scale features of the deposited film can be observed as recorded in a tapping mode.

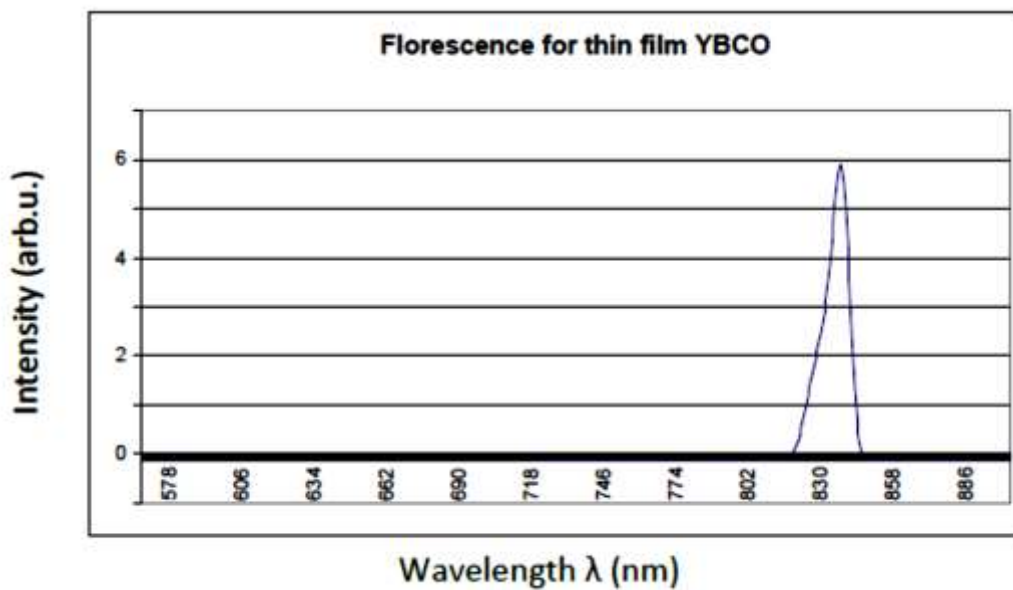


Figure 11. Fluorescence of superconductive  $Y_2Ba_4Cu_8O_{20-x}$  thin film at a wavelength of  $\sim 830$  nm.

#### 4. Conclusions

We successfully fabricated superconductive YBCO nano-layer films by Pulsed laser deposition (PLD) technique based on femtosecond (*f.s.*) provide with 2 amplifiers (800 nm, 40 *f.s.* pulses duration, 1000 Hz repetition rates, 0.3– 0.75 mJ), on a quartz substrate. Superconductor pellets (target) of  $Y_1Ba_2Cu_3O_{6.96}$  and  $Y_1Ba_2Cu_3O_{6.78}$  shows an orthorhombic structure as being evident from the crystallographic splitting of (013), (103)/ (110), and (020), (006), and (116)/ (123), (213). The oxygen content ( $\delta$ ) was determined by iodometric titration method. EDX spectrum shows only O, Cu and Y peaks caused by X-rays given off as electrons return to the K electron shell and one peak resulting from the L shell of Ba. No undesired phases were detected confirming that the target structure is an orthorhombic single phase. Resistivity measurements revealed a transition temperature  $T_c^{onset} = 90$  K with a transition width  $\Delta T_c = 2.0$  K. The zero resistance is achieved at  $T_c(0) = 88$  K. For  $Y_1Ba_2Cu_3O_{6.96}$ , the five z-polarized Raman phonons exist. Raman spectrum containing the five fundamental modes of vibration at 115, 150, 340, 440 and 500  $cm^{-1}$  frequency has been demonstrated. This spectrum confirms the results of oxygen stoichiometry, the phase purity and c-axis orientation of the target materials. Raman spectroscopy is a sensitive tool for detecting the composition, in particular oxygen content, the detection of foreign phases, and the orientation of HTSC materials.

The superconducting PLD-YBCO nano-layer films on a quartz substrate have been deposited at 400°C without post-annealing and with an *ex-situ* annealing in

a flow rate of pure oxygen, for oxygenation, at 950 °C for 18 h. The crystalline structure of the PLD nano films are identified as  $Y_2Ba_5Cu_7O_x$  and  $Y_2Ba_4Cu_8O_{20-x}$ , respectively, as revealed by XRD and EDX measurements. EDX analysis confirmed the phase purity and the absences of impurity phases in the ablated films. Thickness of the deposited film is found to be  $\sim 150$  nm as measured by Fizeau interference (*FI*) technique at reflection, with a deposition time of 10 min.

SEM micrographs of the surface of  $Y_2Ba_4Cu_8O_{20-x}$  thin film deposited at different target-substrate distance ( $d_{T-S}$ ) shows droplets, at  $d_{T-S} = 20$  mm, come from the drawback of PLD which are typically observed in the film surfaces prepared by PLD technique. In contrast, a dense smoother surface structure in a unique orientation was observed for thin film deposited under the optimized condition of  $d_{T-S} = 70$  mm.

AFM scan recorded in a tapping mode of the ablated  $Y_2Ba_4Cu_8O_{20-x}$  surface showed that the film starts to have some atomic arrangements after laser ablation treatments. The particles grain size is found to be 100 - 300 nm as estimated from AFM line profile. Finally, the fluorescence of  $Y_2Ba_4Cu_8O_{20-x}$  thin film shows the emission of a spectral line at a wave length of  $\sim 830$  nm in the I.R region. Based on that fact, this property could be used as a finger print characterizing the deposited oxide thin superconducting films. This information will be useful particularly in the fabrication of high  $T_c$ -device. At last, the laser deposition technique has been proven to be a viable method in producing high quality superconducting films. By using PLD technique, we can fabricate films

of nano-superconducting layers having the same chemical structure as the target material. PLD offers numerous advantages, including film stoichiometry, high deposition rate, low contamination level and non-equilibrium processing. Moreover, accessible experimental parameter is very easy for the synthesis of high temperature superconducting thin films.

#### Acknowledgements

The authors wish to thank the Director and members of the National Research Center, Dokki, Egypt, for providing the PLD technique and maintenance support necessarily for this study. The SEM, EDX and AFM are done in Material Geological Research Center, Giza, Egypt. We also thank Professor M. Dawood in Faculty of Engineering, Menoufia University, for helping in (R-T) measurements.

#### Corresponding author.

Name: M. I. Youssif

Address: Physics Department, Faculty of Science, Damietta University, New Damietta 34517, Egypt

E-mail address: [youssifm@yahoo.com](mailto:youssifm@yahoo.com)

Mobile: +20-01280059909; Fax: +20-057-2403866.

#### References

1. Proc. European Conferences on Applied Superconductivity, Inst. Phys. Conf. Series 158, Vol. 1 (1997).
2. Proc. Applied Superconductivity Conferences, IEEE Transact. Appl. Supercond. 9, No. 2 June (1999).
3. J. A. Greer "In-situ growth of YBCO thin films on three inch wafers using laser ablation and an atomic oxygen source "in: Superconductivity and Applications, H. S. Kwok, Y. H. Kao and D.T. Shaw, Eds. (Plenum Press, New York, 1989) pp. 117 - 126.
4. A. D. Berry, D. K. Gaskill, R. T. Holm, E. J. Cukauskas, R. Kaplan, and R. L. Henry, Appl. Phys. Lett. 52(20), 1743 (1988).
5. P. N. J. Zhao, Materials Science Forum (1993), 130-132: p. 233-254.
6. R. J. Mensah, G. Majkic, Y.M. Chen, V. Selvamanickam, P. Putman, and K. Salama, IEEE Trans. Appl. Supercond. 19(3), 3216 (2009).
7. B. J. Kim, S.W. Lim, H.J. Kim, G.W. Hong, and H.G. Lee, Physica C 445, 582 (2006).
8. M. Klee, W. Brand, and J. W. C. Devries, J. Crystal Growth 91(3), 346 (1988).
9. C. Dubs, K. Fischer, and P. Gornert, J. Crystal Growth 123(3-4), 611 (1992).
10. C. Y. Cho, D. Hwang, K. S. No, J. S. Chun, and S. H. Kim, J. Mater. Sci. 28(11), 2915 (1993).
11. T. Aytug, M. Paranthaman, E. D. Specht, Y. Zhang, K. Kim, Y. L. Zuev, C. Cantoni, A. Goyal, D.K. Christen, V. A. Maroni, Y. Chen, and V. Selvamanickam, Supercond. Sci. Technol. 23(1), (2010).
12. Y. H. Kim, C. J. Kim, B. H. Jun, T. H. Sung, Y. H. Han, S. C. Han, H. J. Paik, J. S. Youn, and K. No, Physica C 469(15-20), 1410 (2009).
13. O. Stadel, R. Y. Muydinov, G. Brauer, M. O. Rikel, J. Ehrenberg, J. Bock, G. Kotzyba, R. Nast, W. Goldacker, S. V. Samoylenkov, and A. R. Kaul, IEEE Trans. Appl. Supercond. 19(3), 3160 (2009).
14. S. Sathyamurthy and K. Salama, Physica C 329(1), 58 (2000).
15. M. Paranthaman, M. S. Bhuiyan, S. Sathyamurthy, H. Y. Zhai, A. Goyal, and K. Salama, J. Mat. Res. 20(1), 6 (2005).
16. A. Gupta, R. Jagannathan, E. I. Cooper, E. A. Giess, J. I. Landman, and B. W. Hussey, Appl. Phys. Lett. 52(24), 2077 (1988).
17. Y. Iijima, N. Tanabe, O. Kohno, and Y. Ikeno, Appl. Phys. Lett. 60(6), 769 (1992).
18. K. Kakimoto, Y. Sugawara, T. Izumi, and Y. Shiohara, Physica C 334(3-4), 249 (2000).
19. L. H. Perng, T. S. Chin, K.C. Chen, and C.H. Lin, Supercond. Sci. Technol. 3(5), 233 (1990).
20. H. J. Scheel, C. Klemenz, F. K. Reinhart, H. P. Lang, and H. J. Guntherodt, Appl. Phys. Lett. 65(7), 901 (1994).
21. J. Tsujino, N. Tatsumi, and Y. Shiohara, Physica C 235, 583 (1994).
22. S. Yuhya, K. Kikuchi, Y. Shiohara, K. Terashima, and T. Yoshida, J. Mat. Res. 7(10), 2673 (1992).
23. J. R. Ahn, S. G. Lee, Y. S. Hwang, G. Y. Sung, and D. K. Kim, Physica C 388, 127 (2003).
24. D. Dijkamp, T. Venkatesan, X. D. Wu, S. A. Shaheen, N. Jisrawi, Y. H. Min-Lee, W. L. McLean, and M. Croft, Appl. Phys. Lett. 51, 619 (1987).
25. H.S.Kwok, P. Mattocks, D. T. Shaw, L. Shi, X. W. Wang, S. Witanuchi, Q. Y. Ying, J. P. Sheng and P. Bush, Mat. Res. Soc. Symp. Proc. 99, 735 (1988).
26. D. B. Geohegan, D. N. Mashburn, R. J. Culbertson, S. J. Pennycook, J. D. Budai, R. E. Valiga, B. C. Sales, D. H. Lowndes, L. A. Boatner, E. Sonder, D. Eres, D. K. Christen, and W. H. Christie, J. Mater. Res. 3(6), 1169 Nov/Dec (1988).
27. I. Ono, Y. Ichino, Y. Yoshida, M. Yoshizumi, T. Izumi, Y. Shiohara, Physics Procedia 27, 216 (2012).
28. S. Adachi, N. Inoue, T. Sugano, K. Tanabe, J. Mater. Sci. Lett. 21, 669 (2002).
29. Hanyu S, Miura T, Iijima Y, Igarashi M, Hanada Y, Fuji H, et al., Journal of Physics 97, 012273 (2008).

30. K. Moorjani, J. Bohandy, F. J. Adrian, B. F. Kim, R. D. Shull, C. K. Chiang, L. J. Swartzendruber, and L. H. Bennett, *Phys. Rev. B* 36, 4036 (1987).
31. D. N. Mashburn, D. B. Geohegan, D. Eres, D. H. Lowndes, L. A. Boatner, B. C. Sales, S. J. Pennycook, R. J. Culbertson, E. Sonder, and D. K. Christen, *Mat. Res. Soc. Symp. Proc.* 99, 699 (1988).
32. T. Venkatesan, X. D. Wu, A. Inam, and J. B. Wachtman, *Appl. Phys. Lett.* 52, 1193 (1988).
33. M. Lorenz, H. Hochmuth, D. Natusch, H. Börner, T. Thärigen, D. G. Patrikarakos, J. Frey, K. Kreher, S. Senz, G. Kästner, D. Hesse, M. Steins, W. Schmitz, *IEEE Transact. Appl. Supercond.* 7(2), 1240 (1997).
34. Adam Mann, "High-temperature superconductivity at 25: Still in suspense", *Nature* (Jul 20, 2011); 475(7356):280-2.
35. P. Monthoux, A. V. Balatsky, and D. Pines, *Phys. Rev. Lett.* 67, 3448 (1991).
36. S. Nakajima, M. Kikuchi, Y. Syono, T. Oku, D. Shindo, K. Hiraga, N. Kobayashi, H. Iwasaki, Y. Muto, *Physica C* 158 (1987) 471.
37. M. I. Youssif, and A. Sedky, *Journal of American Science* 11(7), 42 (2015).
38. Evan H. Appelman, Lester R. Morss, Aravinda M. Kini, Urs Geiser, A. Umezawa, G. W. Crabtree, K. Douglas Carlson, *Inorg. Chem.* 26 (20), 3237 (1987).
39. Lotfi Z. Ismail, Mortady I. Youssif, Hussein M. Abdel Moneim, *J. Phys. Chem. Solids* 64, 1405 (2003).
40. D. William. John, "Measurement of Film Thickness," In *Handbook of X-rays*, Edited by Emmett F. Kaelble, McGraw-Hill, New York, 1967.
41. A. Sedky, M.I. Youssif, S. M. Khalil, Ayman Sawalha, *Solid State Communications* 139, 126 (2006).
42. P. H. Hor, R. L. Meng, Y. Q. Wang, L. Gao, Z. J. Hung, J. Bechtold, K. Foster and C.W. Chu, *Phys. Rev. Lett.* 58, 1891 (1987).
43. M.N. Lliev, *Spectroscopy of Superconducting Materials*, ACS Symposium Series 730, in: E. Faulques (Ed.) American Chemical Society, Washington DC (1999) p. 107.
44. Y. -A. Jee, M. Li, B. Ma, V. A. Maroni, B. L. Fisher, U. Balachandran, *Physica C* 356, 297 (2001).
45. S. Adachi, N. Inoue, T. Sugano, K. Tanabe, *J. Mater. Sci. Lett.* 21, 669 (2002).

4/13/2016